Machine learning for epileptic seizure detection

A Research Project presented by
Jessica Uppal

For the degree of BSc (Hons) Neuroscience

School of Life and Health Sciences
Aston University

23rd April 2022

Supervisor: Dr John Butcher

Contents

Abstract
Epilepsy is a neurological disorder characterised by two or more unexplained seizures, disrupting everyday life for patients suffering from this chronic condition (Stafstrom & Carmant., 2015). Currently, around thirty percent of patients are not responding to drug therapy (Schmidt and Schachter, 2014), and despite the many non-pharmacological options available for controlling seizures, such as the ketogenic diet, epilepsy surgery, and neuromodulatory devices such as vagus nerve stimulation (VNS), a large percentage of patients continue to suffer from uncontrolled seizures (Sirven, 2015). With the advancement of artificial intelligence and an era where technology and healthcare can coexist, automated seizure prediction techniques could benefit not only epilepsy patients but also family, caregivers, and medical personnel and alleviate socioeconomic burdens (Pugliatti *et al*., 2007). For the first time, this paper proposes a deep learning Long short-term memory (LSTM) network model with MATLAB R2021b for automatic prediction of epileptic seizures based on local field potential data. The model was trained on a labelled dataset of seizure and non-seizure data, and three unseen test channels were used to perform a preliminary evaluation of model performance. Model parameters were chosen based on similar studies and through trial and error; however, the LSTM model is a 'black-box' approach making it a challenge to ensure that the model has been optimised effectively. The model was most effective at 40 epochs, where it produced an average classification accuracy of 98.8%, sensitivity of 38.7%, specificity of 99.2%, precision of 22.9%, and an F1 score of 0.3. Despite the model's successful accuracy and specificity scores, a critical examination of machine learning algorithms and comparison with existing literature revealed the model's several limitations. These limits include a significant class imbalance, where the number of non-seizure events in comparison to seizure events was significantly out of proportion, and its failure to detect pre-ictal seizure events at a lower number of epochs. In view of this, there is scope for improving the model to both enhance the performance of early seizure detection and produce reliable results before a further application can be considered. Using this model as a foundation, future research can improve and possibly develop real-life algorithms to improve the quality of life for patients with uncontrollable seizures.

Introduction

The Greek phrase "to seize upon" is thought to be the origin of the word epilepsy, where its history and treatment date back at least 4000 years (Reynolds, 2009). Previously, epilepsy's cause was widely believed to be the result of evil influences, where it was once viewed as being the result of "the hand of sin," as quoted in ancient Mesopotamian texts (Panteliadis *et al*., 2017). Pathophysiological theories later identified the brain as essential in epilepsy, although it was thought that the disorder stemmed from excess brain phlegm (Patel & Moshé., 2020). Epilepsy is thought to have affected numerous prominent historical figures such as Julius Caesar and Napoleon I for much of history, having long-term societal consequences (Ali *et al*., 2016). Today it recognised as a clinical condition characterized by two or more unexplained seizures (Stafstrom & Carmant., 2015), although not all seizures may be related to epilepsy, for example, drug-induced seizures (Manford, 2017). Despite the mounting attention epilepsy has received over the centuries, advancements in effective treatment options have only been made in the last half-century.

Aetiology and treatment of epilepsy

While epilepsy's cause remains unclear, research suggests it may be influenced by genetics (Steinlein., 2008) or damage to the brain (Sirven, 2015). Stroke is the single most common cause of epilepsy among adults, while the least common and preventive risk factor is a traumatic brain injury. A cerebral infection may also lead to epilepsy, a prevalent problem in developing countries. Other possible causes include autoimmune disorders such as type I diabetes mellitus (Chou et al., 2016) and alcohol may be associated with dose-dependent epilepsy (Hillbom, Pieninkeroinen and Leone, 2003). Low oxygen levels during birth may also contribute to epilepsy.

The need for automated real-time seizure prediction is motivated by the 65 million people worldwide who have epilepsy (Ngugi *et al*., 2010), thirty percent (WHO, 2018) of whom have not been able to gain control of their seizures despite the novel anticonvulsant drugs that have been introduced to the market in the last decade (Shoeibi *et al*., 2021). In addition, approximately one-third of patients who

initially respond to antiepileptic drugs progress to drug-resistant epilepsy, presenting with refractory seizures (Sirven, 2015), making the development of an automatic seizure detecting model even more critical (Needs *et al*., 2019).
Nonpharmacological treatments have also been introduced, such as the ketogenic diet. This has been mainly used in paediatric epilepsy, showing over 50% reduction in seizures (Henderson *et al*., 2006). VNS is another nonpharmacological intervention that reduces seizures by sending regular, mild pulses of electrical energy to the brain via the vagus nerve. Epilepsy surgery is also available for drug-resistant patients offering a 70% success rate (West *et al*., 2019). However, this treatment is invasive and has high risks, such as possible damage to the eloquent cortex along with the general risks associated with surgery. Patients who may be unwilling or ineligible to go through invasive surgery or have had little success with antiepileptics could benefit from receiving warnings on impending seizures, enabling them to prepare and consider their safety and better manage their epilepsy (Rasekhi *et al*., 2013).

Generalised and focal onset seizures
There are two major types of epileptic seizures: generalized onset and focal onset. Generalised seizures are distinguished by a complete loss of consciousness at the beginning of the convulsion since the entire cortex is involved (Siddiqui *et al*., 2020). Focal seizures can be further categorised into complex and simple partial seizures, both caused by neuronal networks isolated to a portion of the cerebral hemisphere (Stafstrom & Carmant., 2015). Simple partial seizures do not cause any change in consciousness, while complex partial seizures do (Fisher, 2017). Furthermore, epilepsy is believed to have a bimodal incidence distribution, with both infants and older adults being at higher risk (England *et al*., 2012). In addition, the types of seizures that occur in these two groups differ, with generalized seizures being more prevalent in children and partial seizures more prevalent in adults (Beghi, 2020).

Seizure stages
Four main stages are identified during epileptic seizures: pre-ictal, ictal, post-ictal, and inter-ictal (Fisher *et al*., 2014). Pre-ictal refers to the period preceding the seizure, ictal refers to the interval during the seizure, post-ictal refers to the period following the seizure, and inter-ictal refers to the interval between two seizures (Figure 1). An effective seizure prediction system would need to distinguish between pre-ictal and inter-ictal states, with the detection of the pre-ictal phase as early as possible (Abbasi *et al*., 2019).

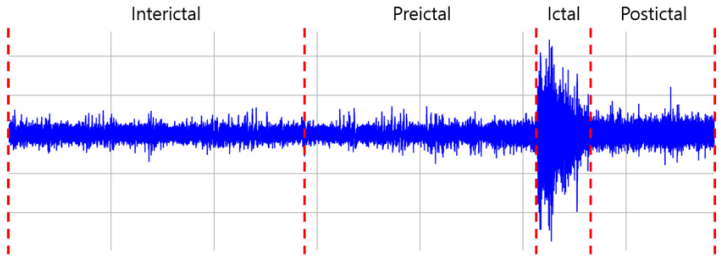

Figure 1. Epileptic brain states displaying interictal, preictal, ictal and postictal stages. The x-axis displays the time, and the y-axis displays the measured voltage. The red lines indicate the start of a new seizure stage (Taken From: Ryu and Joe., 2021).

Introduction to machine learning and neural networks
Artificial intelligence in healthcare is powered by machine learning (ML) which refers to algorithmic software that can detect patterns in huge datasets (Sone & Beheshti, 2021). Several recent projects involving ML have produced impressive results in areas of medical support (Cutillo *et al*., 2020), including patient monitoring and clinical decision support (Rowe., 2019). A subset of ML known as deep learning utilises neural networks, which include convolution neural networks (CNN), artificial neural networks (ANN), and, importantly, recurrent neural networks (RNNs). RNNs comprise of three layers: an input layer, hidden layers, and an output layer (Figure 2). The hidden layer's output is identified using the current layer's input and the previous layer's output, allowing the algorithm to

recognize relationships among datasets similarly to how the human brain functions (IBM Cloud Education, 2020). This structure allows the RNN to acquire the ability to recall historical outcomes and exchange data among the hidden layers. (Maragatham and Devi, 2019). It is particularly important in time-sequence datasets such as the one presented in this study because the network is able to form connections even when there is a long lag of unknown size (Gagliano et al., 2019).

A famous drawback of RNNs is that they perform poorly when dealing with long sequences such as electroencephalography (EEG) recordings due to their gradient vanishing and exploding. LSTMs seek to address this issue by using a gated mechanism that includes a forget gate, an input gate, and an output gate (Bongiorni & Balbinot, 2020). The LSTM model is an RNN technique proposed by Hochreiter and colleagues in 1997. It has since been used in seizure detection by Ahmedt-Aristizabal and co-workers (2018) and Hussein and colleagues (2018), who proposed a robust epilepsy detection system with LSTM capable of handling noisy EEG data. Neither study, however, has used LFP data. Further analysis of machine learning algorithms for epileptic seizure detection by Lekshmy and colleagues (2022) has revealed that the random forest and LSTM outperform other models in terms of sensitivity and specificity. However, this is determined by the model's optimisation methods. The authors also specified that LSTM is more suitable for time-series data, producing high accuracy, while random forests are better suited to supporting a variability of data.

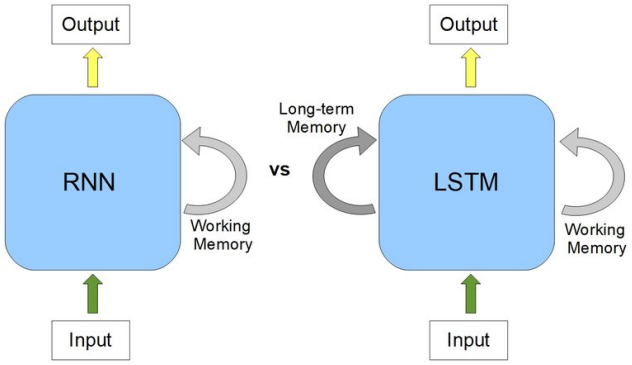

Figure 2. RNN and LSTM comparison. RNN demonstrates a use of their internal state (memory) to process sequences of inputs. The LSTM network has an additional long-term memory component to remember past data (Taken from: Yasrab and Pound., 2020).

Importance of machine learning in seizure detection

Clinical trials involving implantable automated seizure controlling devices have been carried out since the early 1980s (Stacey & Litt, 2008); while many studies have been published since, a successful device has not yet been introduced to the market (Tang *et al*., 2021). It is hypothesised that a machine learning model capable of detecting and learning seizure patterns could be used alongside neurostimulators to prevent seizures, thus enabling automated seizure control for patients (Lekshmy *et al*., 2012).

The chance of untimely death associated with epilepsy is nearly three times greater than healthy people (World health organization, 2019). This is linked to people with epilepsy being at a higher risk of facing life-threatening incidents linked to seizures. Although some patients may experience an aura, many epileptic seizures occur without warning, leaving no time for patients to consider their surroundings and safety (Beghi, Giussani and Sander, 2015). The highest risk is associated with generalised atonic seizures (Siddiqui *et al*., 2020), also known as drop attacks, where consciousness is lost. Among the most feared epilepsy-related injuries is submersion injuries, motor vehicle accidents, burns, and head trauma (Nguyen & Téllez Zenteno., 2009). Therefore, seizure detection is paramount, especially for vulnerable groups such as the elderly, who may be more prone to fractures, and pregnant women. The unambiguity of seizure episodes can cause constant worry, severely impacting daily life and exerting a detrimental effect on mental health. This notion is supported by a study conducted by Lu and colleagues (2021), who found a positive correlation between seizure frequency and suicidal ideation. Furthermore, seizures can have lasting effects on patients' relationships and

professional life (Mlinar *et al*., 2016). For example, in the United Kingdom, people must be seizure-free for at least 12 months before driving, often resulting in inactivity, isolation, and dependency (Nguyen & Téllez Zenteno., 2009). The economic impact is also staggering, with the NHS spending approximately £1.5 billion per year on epilepsy, with the high costs incurred to assess, treat, perform surgery, and hospitalise patients, as well as secondary effects such as lost employment (sudep.org). This toll is greater across Europe, with €15.5 billion per year spent on epilepsy (Pugliatti *et al*., 2007), projected to have increased up to present times. To date, studies have offered few strategies to reduce the financial impact of epilepsy, an issue that must be addressed.

An automatic seizure detection system could further support healthcare professionals as manual detection is time-consuming, costly, and subject to bias (Guo *et al*., 2010). This can reduce the mounting pressure on the worldwide healthcare system, already strained by increasingly common neurological disorders like Alzheimer's and the recent COVID-19 pandemic.

LFPs and seizure detection

Although studies have previously evaluated seizure detection using EEG data which serves as the gold standard for epilepsy diagnosis due to its non-invasive nature (Hussein *et al*., 2018), little has been published using electrophysiology data despite its several advantages. LFPs are electric potentials measured in depth from the extracellular space within cortical tissue using micro-electrodes (Buzsáki *et al*., 2012). This allows them to sample a more local population of neurons, unlike EEGs, which do not indicate seizure localisation and show seizure activity only after spreading to the cerebral cortex (Smith, 2005). LFPs recorded at the epicentre of a seizure can also significantly improve the performance of seizure-predicting algorithms and could be a valuable tool to use alongside epilepsy surgery for seizure localisation. This feature is critical as the efficacy of the surgery depends significantly upon successful seizure localisation of the epileptogenic zone (Zare et al., 2020, Aghagolzadeh *et al*., 2016). This, however, comes at the expense of invasive surgery, making LFP data difficult to obtain from humans.

EEGs are often contaminated by muscular (EMG) activity and distorted by the filtering and attenuation produced by the intervening layers of cerebrospinal fluid, tissue, skull, and scalp (Anastasiadou *et al*., 2014). This not only makes it less effective in seizure detection using ML but also makes it difficult for physicians to diagnose epileptic seizures. Although EEG studies have clear disadvantages, the results obtained are often valid because noise and unwanted signal components are removed during pre-processing, increasing the Signal-to-Noise Ratio (SNR) (Usman *et al*., 2017). On the contrary, pre-processing must be minimal to benefit from automatic seizure detection. The model should be trained to automatically identify features from the raw signal, reducing the need for specialists to perform tedious feature design.

Aim and Objectives

This project aimed to develop an algorithm that can automatically and accurately detect seizures based on an LFP dataset containing seizure and non-seizure events. The objectives were to demonstrate that seizure and non-seizure samples can be correctly classified using the model's features with high accuracy, predict seizure events before they occur, and provide a basis of warning for potential real-world application of detecting seizures.

To achieve these objectives, optimization methods were used to obtain an accurate performance to enable the model to detect seizures before they occur.

Methods

LFP Seizure protocol

Male Wistar rats that had previously been subjected to the Reduced Intensity Status Epilepticus (RISE) model of temporal lobe epilepsy were used to prepare the slices. The age of the animal used was determined by the experimental objectives. Local field potential (LFP) recordings were made on 450 μm thick slices.

To prepare for brain extraction, each animal was first anaesthetised using 5% isoflurane in N2/O2. The animals were then given pentobarbital (600mg/kg) subcutaneously (SC) and ketamine (100mg/kg) and xylazine (10mg/kg) intramuscularly (IM) to induce terminal anaesthesia and neuroleptanalgesia. To determine the correct depth of anaesthesia, the absence of normal paw pinch and corneal reflex was used. The animals were immersed in ice-cold water for 45 seconds before receiving transcranial perfusion with 20 – 40ml of ice-cold sucrose-based artificial cerebrospinal fluid (aCSF, cutting solution) containing (in mM): 180 sucrose, 2.5 KCl, 10 MgSO4, 1.25 NaH2PO4, 25 NaHCO3, 10 glucose, 0.5 CaCl2, 1 L-ascorbic acid, 2 N-acetyl-L-cysteine, 1 taurine and 20 ethyl pyruvate.
To improve slice viability, neuroprotectants including (in mM): 0.045 indomethacin (a cyclo-oxygenase (COX-2) inhibitor (Asanuma *et al.*, 2001)), 0.2 aminoguanidine (a nitric oxide synthase (iNOS) inhibitor (Griffiths *et al.*, 1993)), 0.4 uric acid (an anti-oxidant (Proctor, 2008), 0.13 ketamine (non-competitive NMDAR antagonist (MacDonald *et al.*, 1991)) and 0.2 brilliant blue G (a P2X7 antagonist and anti-inflammatory agent (Peng *et al.*, 2009)) were added to the cutting solution. The complete cutting solution was saturated prior to perfusion with 95% O2/5% CO2 (carbogen), pH 7.3, 300 – 310 Osm/L.
The brain was placed in the remaining cutting solution for transportation following rapid dissection and extraction of the brain. Slicing was performed at room temperature in the ice-cold cutting solution using a 7000smz-2 model Vibrotome (Campden Instruments Ltd). Horizontal or coronal slices were made to contain the hippocampus/mEC or mPFC, respectively. The slices were then transferred to the holding chamber and stored at room temperature for one hour in a standard aCSF containing (in mM): 126 NaCl, 2.5 KCl, 1 MgCl2, 2.5 CaCl2, 26 NaHCO3, 2 NaH2PO4 and 10 D-glucose. Neuroprotectants were also added (in mM): 0.045 indomethacin and 0.4 uric acid. A continuous perfusion of 95 percent O2/5 percent CO2 (carbogen) assisted in maintaining a pH of 7.3 and an oxygen saturation of 300 – 310 Osm/L.

Slices being used for extracellular recordings were transferred onto the LFP rig which contained an interface chamber (Scientific Systems Design Inc, Canada), following one-hour recovery in the holding (interface) chamber. Slices were perfused continually with saturated NaCl-based aCSF (95% O2/5% CO2 (carbogen)) at a flow rate of 5-6ml/min and temperature of 30–33ºC using a proportional temperature controller PTC03 (Scientific Systems Design Inc, Canada). Microelectrodes were pulled from borosilicate glass (1.5mm diameter, Warner Instruments, USA) at a resistance of 3 – 5 MΩ using a PC-10 micropipette/microelectrode puller (Narishige Ltd, Japan). These microelectrodes were filled with NaCl-based aCSF before a chloride coated silver wire was inserted and placed in one of the four headstages.
The microelectrodes were lowered into the slice using the MM-3 micromanipulator (Narishige Ltd, Japan) with the aid of the rat brain atlas under the supervision of an Olympus SZ51 (Olympus, UK) stereomicroscope (Paxinos and Watson, 1998). CA1 and CA3 of the hippocampus were implanted with microelectrodes. Depending on the experiment, drugs were also bath applied and perfused onto the slices. In the case of seizure generation, baseline activity was recorded for 30 minutes in normal aCSF before switching to the same aCSF containing 0 mM MgCl2. If the brain slices failed to generate repetitive seizures after 3 hours, the potassium concentration in the bath solution was increased to 6 mM total. This usually resulted in the occurrence of a recurring seizure pattern.

To visualise the recording, the voltage signal was first amplified x100 with an EX10-2F amplifier (NPI Electronics GMBH, Germany) equipped with a 0.1 Hz high-pass filter and a 1 KHz low-pass filter. Hum bugs were used to filter 50 Hz electrical noise (Quest Scientific, Canada). The signal was amplified x20 using an LHBF-48X amplifier (NPI Electronics GMBH, Germany) with a 0.3 Hz high-pass filter and a 700 Hz low-pass filter. The signal was then digitised at 5 KHz using a CED Micro1401-4 analogue-to-digital converter (Cambridge Electronic Design, UK) and recorded with Spike2 software (Cambridge Electronic Design, UK).
The signal is the result of the accumulation of transient fluctuations in extracellular ion concentrations. The LFP is generated by local neuronal ensembles that produce current sinks (inward currents) and sources (outward currents) (Mitzdorf, 1985). These currents are generated primarily by synaptic activity (EPSP and IPSP), but they are also influenced by Ca2+ spikes, other voltage-dependent intrinsic events, action potentials, and spike after-potentials. As a result, LFP provides

insight into neuronal cooperative behaviour (Buzsáki, Anastassiou, and Koch, 2012). It is important to note that the tip of the microelectrode has a recording area of approximately 250 µm (Katzner *et al*., 2009), implying that the sampling area is small, especially when compared to other field recording techniques such as EEG, though LFP recording is often referred to as 'tissue' EEG.' (Marley. N., Unpublished) (Wright *et al*., 2020).

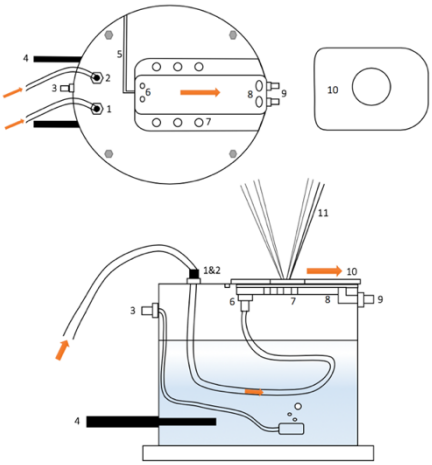

Figure. 3 The local field potential interface recording chamber.
(A) Plan view of the interface chamber aCSF (with circulating drugs) enters through points 1 and 2 before circulating through the interface chamber and exiting through point 6. Slice(s) are placed in the tray's centre and will be saturated by the flow of aCSF. The gas feed in connector is shown in point 3. Point 4 depicts the two heater inputs/feedback centre, which aid in maintaining the temperature between 30-33 °C. Point 5 illustrates the grounding wire guide. Six port holes (point 7) are for the rising humidified gas. Outflow is shown at point 8, which feeds into the drippers at point 9 and allows the aCSF to be recirculated. (B) An acrylic lid is placed over the slices (s). Microelectrodes can be accessed through the central hole. (C) Diagram A, side view. The water level within the interface chamber is also shown, which is bubbled with carbogen via the gas feed in point 3. The perfusion solution feed (1&2) feeds into the water to warm up the aCSF. Through the hole in the acrylic slide, up to four microelectrodes (11) were inserted into the slice(s) at once (10). The flow direction is indicated by orange arrows (Taken from: Marley. N., Unpublished).

Data and model architecture
This project includes eight MATLAB files and four channels (1, 2, 3, and 4), each including a corresponding input and output channel. Each channel comprises of 855,605 data points which are labelled as either seizure or non-seizure in the form of 1 and -1, respectively.
One channel was chosen at random and used for training the model (channel 2) and the remaining three channels were used for testing (channels 1, 3, and 4). All channels had a significant class imbalance where the training channel 2 had only 5946 seizure points, while non-seizure made up 849,659 points. This meant that the seizure detection model was trained on a channel where only 6.9% of the data points were seizures.

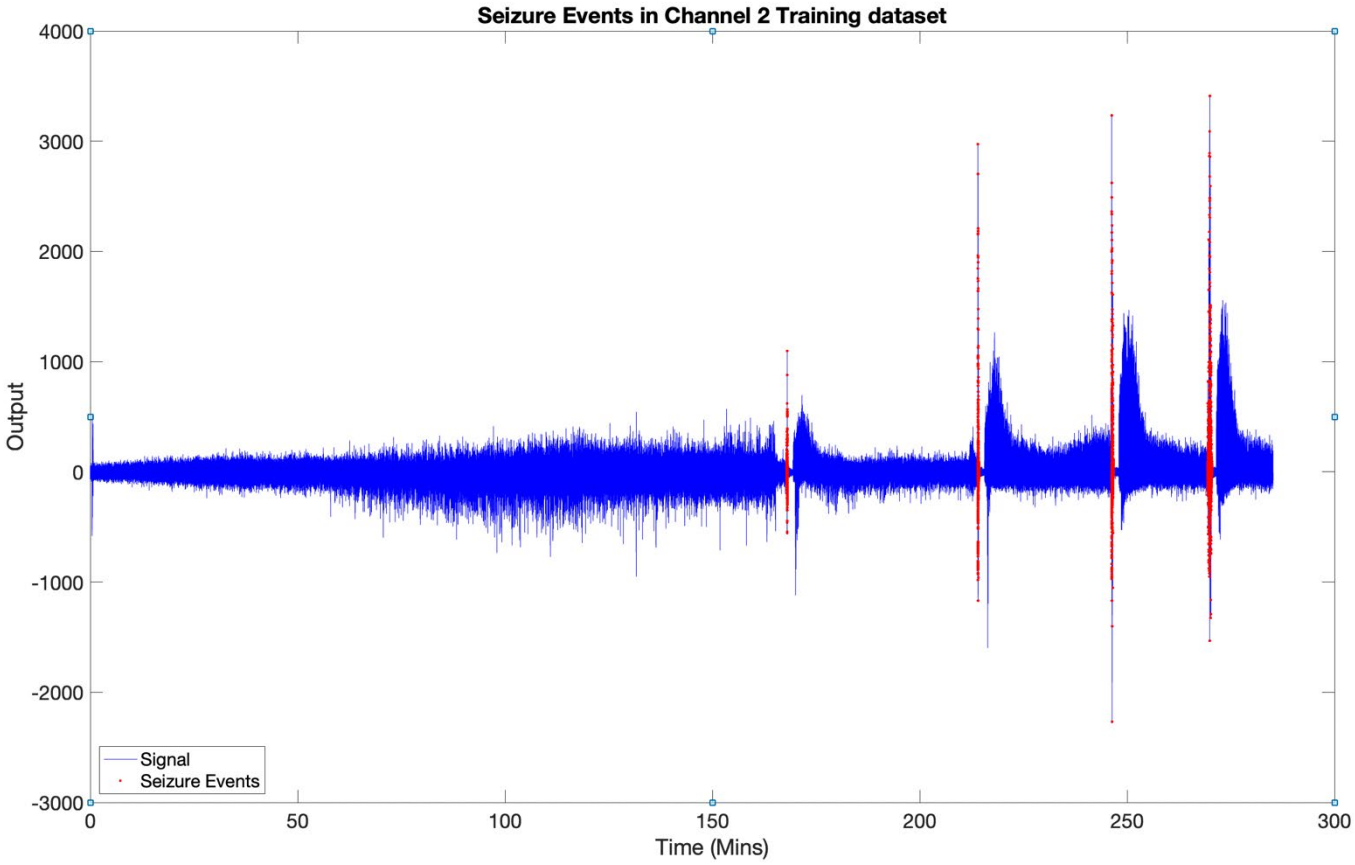

Figure 4. Channel 2 training dataset output. The labelled seizure events are shown in red and are seen as four clear spike events. Non-seizure events are represented in blue. The x axis shows the time of the signal in minutes, which is a total of 285.2 minutes. An artifact is present at the start of the signal at around 1 minute.

Figure 5. LSTM network architecture for classification built using MATLAB Deep Network Designer. The LSTM network compromises of a sequence input layer, LSTM layer, fully connected layer, softmax layer and followed by a classification layer respectively (Figure 4).

The model was trained using the Adam optimiser and built using a sequence input layer that feeds sequence data into a network. The LSTM layer learns the long-term dependencies between time steps (Brownlee, 2018), and the network concludes with a fully connected layer, a SoftMax layer, and a classification output layer to predict class labels (Figure 5). The number of features is one, and the

number of classes is two, corresponding to seizure and non-seizure events. The number of hidden units was set to 200, and the LSTM layer output was set to 'sequence.' Refer to Appendices.

Model training

The model was trained on several epochs ranging from 10 to 80. *Epochs* are a ML hyperparameter that indicates how many passes the machine learning algorithm has made through the entire training dataset (Gaillard, 2020). In one epoch, all samples in the training dataset have had the opportunity to update the model parameters (Brownlee, 2018). The performance of the proposed LSTM models for epileptic seizure detection has been illustrated in terms of loss and accuracy curves during the training process to ensure LSTM stability (Figure 6-8). With increasing epochs, loss curves decay exponentially and converge to the lowest loss value in the training dataset.

Similarly, Figures 6 and 7 depict a rise in classification accuracy with respect to epochs, followed by a plateau. This demonstrates the LSTM model's consistent performance for accurate seizure prediction. For 80 epochs, however (Figure 8), the accuracy was not consistent, as seen by a slight loss of accuracy at around 52 epochs and an increase in loss also at the same point. Again, this pattern could be observed at the end of the 80 epochs, proving that increasing the number of epochs is not always good. This inconsistency may be caused by the same dataset being presented too many times, leading to potential overtraining, and instead of increasing accuracy and decreasing loss, the opposite effect can occur.

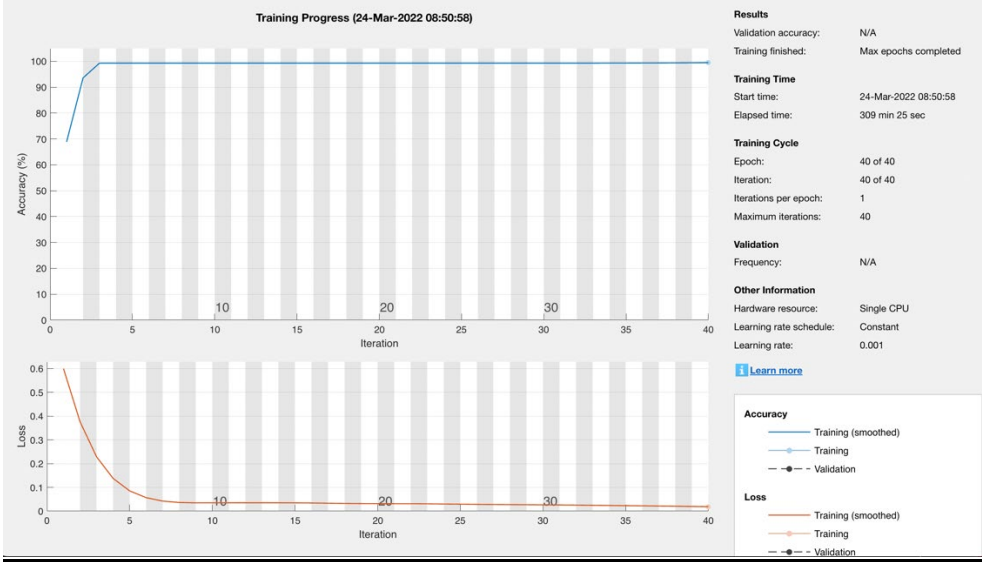

Figure 6. Training progress plot generated by MATLAB at 40 epochs showing accuracy and loss. (A) Accuracy increases from around 70% to almost 100%. Accuracy plateaus after 2 epochs where it remains constant through to 40 epochs. (B) Loss decreases rapidly and becomes steady at around 7 epochs where it remains levels until the end of training at 40 epochs.

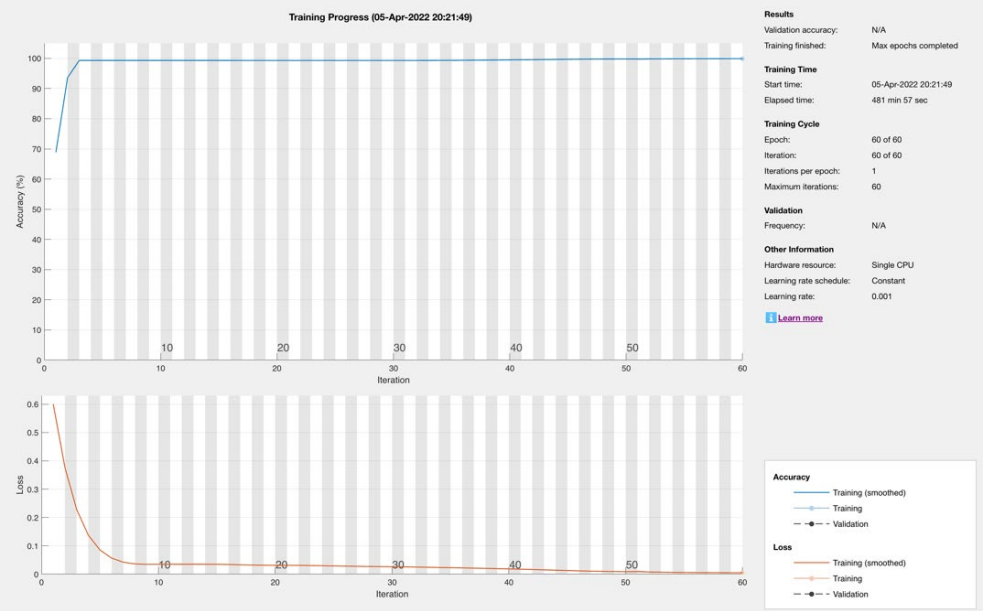

Figure 7. Training progress plot generated by MATLAB at 60 epochs showing accuracy and loss. (A) Accuracy increases from 70% to almost 100%. Accuracy plateaus after 2 epochs where it remains constant through to 60 epochs. (B) Loss decreases rapidly and then slowly at around 6 epochs until reaching the lowest point at 60 epochs.

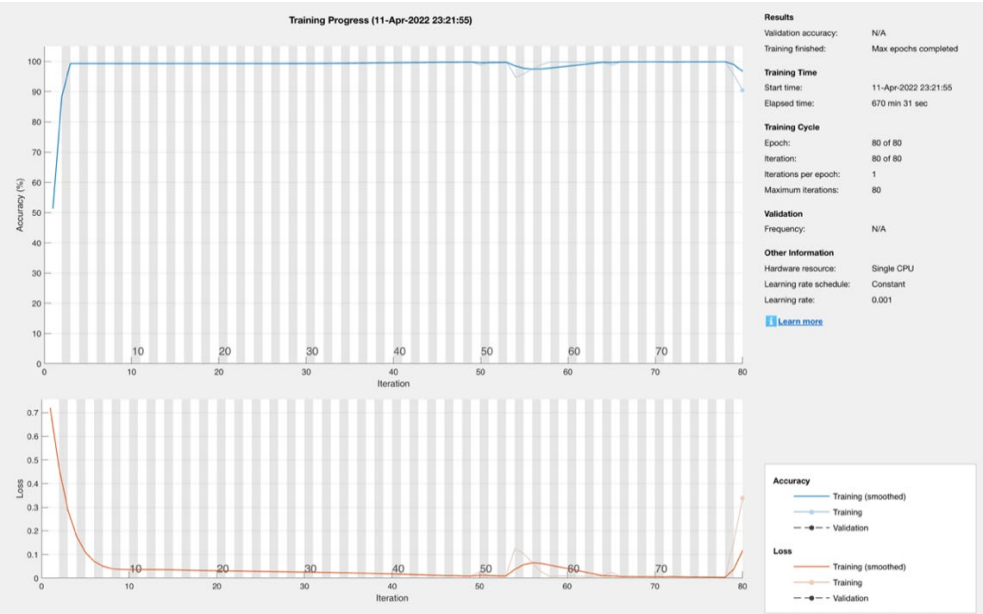

Figure 8. Training at 80 epochs showing accuracy and loss. Plot generated by MATLAB. (A) Accuracy increases around 50% to almost 100%, where its stays stagnant until 52 epochs where a loss in accuracy is observed, this increases again at around 62 epochs and this loss in accuracy is seen again at around 78 epochs. The loss and accuracy plots mirror each other. As accuracy increases, loss decreases and vice versa. (B) Loss decreases rapidly and then slowly, but at 52 epochs small increase which decreases and levels off at 62 epochs. At 78 epochs loss has again increased.

Besides increasing the number of epochs, other methods of optimisation are also possible, although they are usually considered fine-tuning (Almustafa., 2020). Learning rate, for instance, is a configurable parameter set between 0.0 and 1.0 that can influence the convergence of the algorithm. The learning rate was normalised by Adam optimisation as 0.001 (Figure 6-8) and was not adjusted in this training model, as this optimisation is not heavily based on the setting of the learning rate

(Maragatham and Devi, 2019). A higher learning rate means the neuron updates values quickly but may never reach convergence as the sufficient value may be skipped. However, if the learning rate is too low, it may never reach convergence because it only updates the weight minimally (Brownlee, 2019). Generally, a good learning rate should lie between 0.1 and 0.001, where Adam optimisation in activation layers is widely considered the best approach. It routinely normalises this rate without manual adjustment (Abbasi *et al*., 2019). The training time was longest for 80 epochs at 670 minutes and 31 seconds on a laptop with a 3.2GHz Apple M1 processor with an 8-core CPU and 16GB RAM, using MATLAB (Figure 8). For larger sets of data needed to train a model for clinical application, this could take a lot longer, especially at a higher number of epochs, although this would also depend on the machine used and whether it has a GPU (Hunyadi et al., 2017).

Performance Metrics

The following performance metrics were calculated, in addition to accuracy, to facilitate comparisons with other methods described in similar literature. TP (true positive), TN (true negative), FP (false positive), and FN (false negative) values were taken to determine performance. TP refers to seizures that are predicted correctly as seizures. TN refers to non- seizures that a predicted correctly as non-seizures. FP refers to non-seizure events that are falsely predicted as seizure events, and FN refers to seizures that are classified as non-seizures.

$$Accuracy = \frac{TP+TN}{(TP+FP+FN+TN)}$$

$$Sensitivity/Recall = \frac{TP}{(TP+FN)}$$

$$Specificity = \frac{TN}{(TN+FP)}$$

$$Precision = \frac{TP}{(TP+FP)}$$

$$F1\ Score = 2x \frac{Precision\ x\ Recall}{Precision+Recall}$$

Results

Numerous optimisation methods exist in ML, modifying the number of epochs as the most obvious example. A model with more epochs would have a greater time to learn the model and update its weights (Brownlee, 2018). During initial training, ten epochs were used; however, no seizure events were detected, suggesting that training a dataset of this size with ten epochs would not be feasible. The model was then trained in intervals of ten epochs from 20 until 80 epochs had been reached to determine an optimal number. This was done for all three test channels (Figure 9-11).

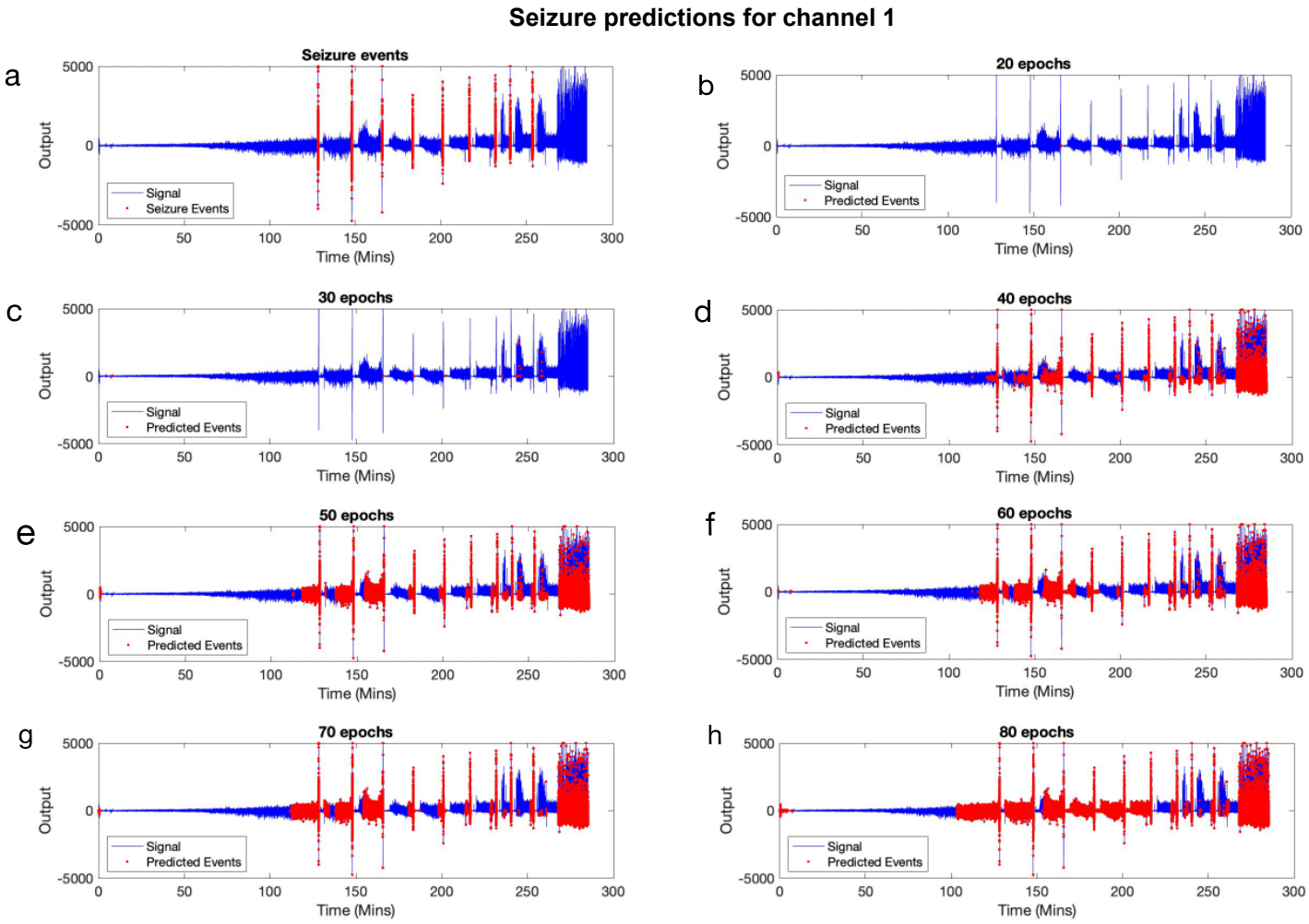

Figure. 9
Model performance for channel 1 using networks trained at an increasing number of epochs. Seizure predictions are illustrated in red, and non-seizure in blue. x-axis is time. Graph (a) shows channel 1 actual seizure events highlighted in red. (b) shows channel 1 tested at 20 epochs (c) at 30 epochs, (d) 40 epochs, (e) 50 epochs (f) 60 epochs, (g) 70 epochs (h) 80 epochs. Total number of seizure points in channel 1 is 9115.

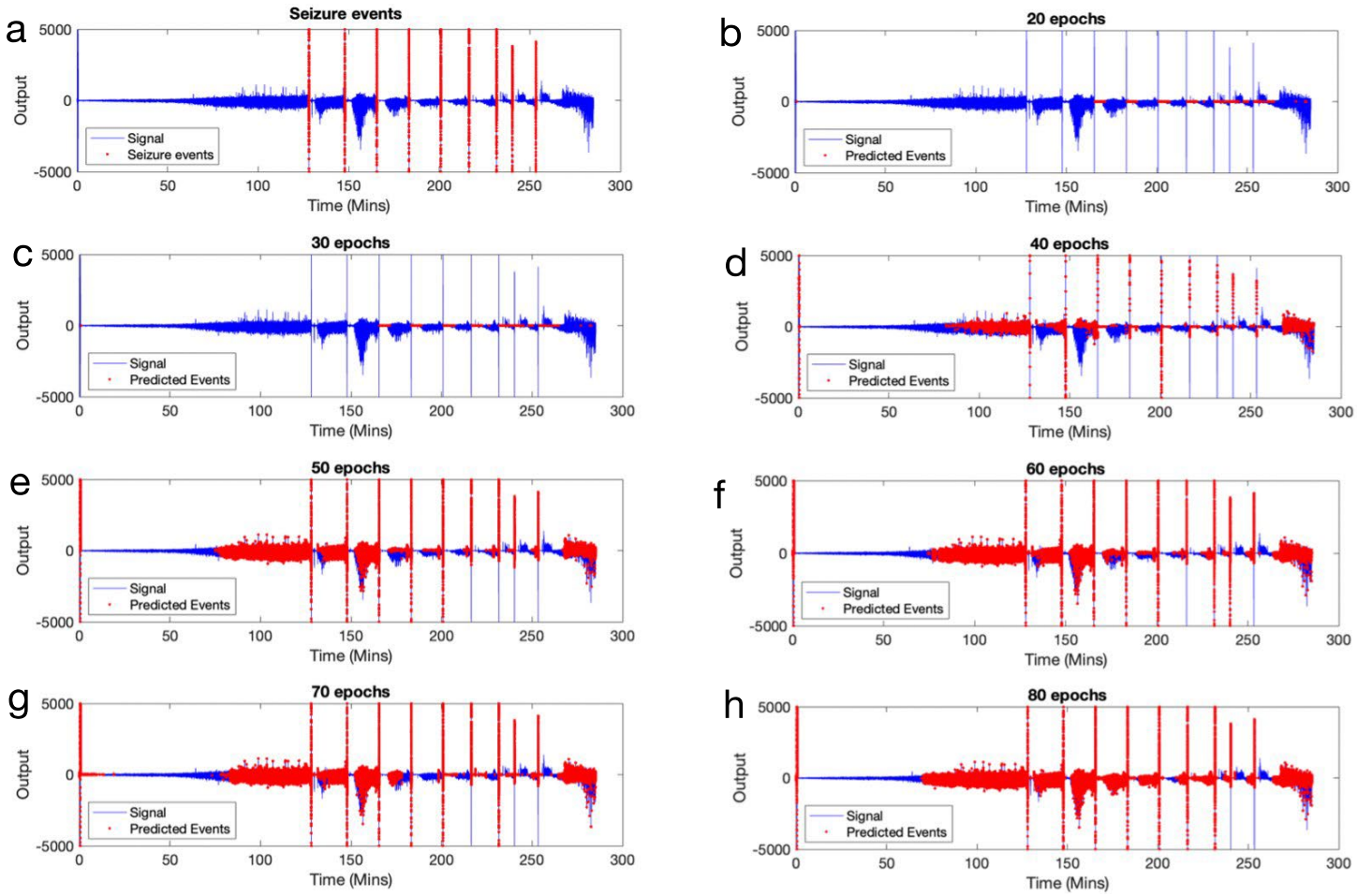

Figure. 10
Model performance for channel 3, using networks trained at an increasing number of epochs. Graph (a) shows channel 1 actual seizure events highlighted in red. (b) shows channel 1 tested at 20 epochs (c) at 30 epochs, (d) 40 epochs, (e) 50 epochs (f) 60 epochs (g) 70 epochs and (h) 80 epochs. Total number of seizure points in channel 3 is 4150.

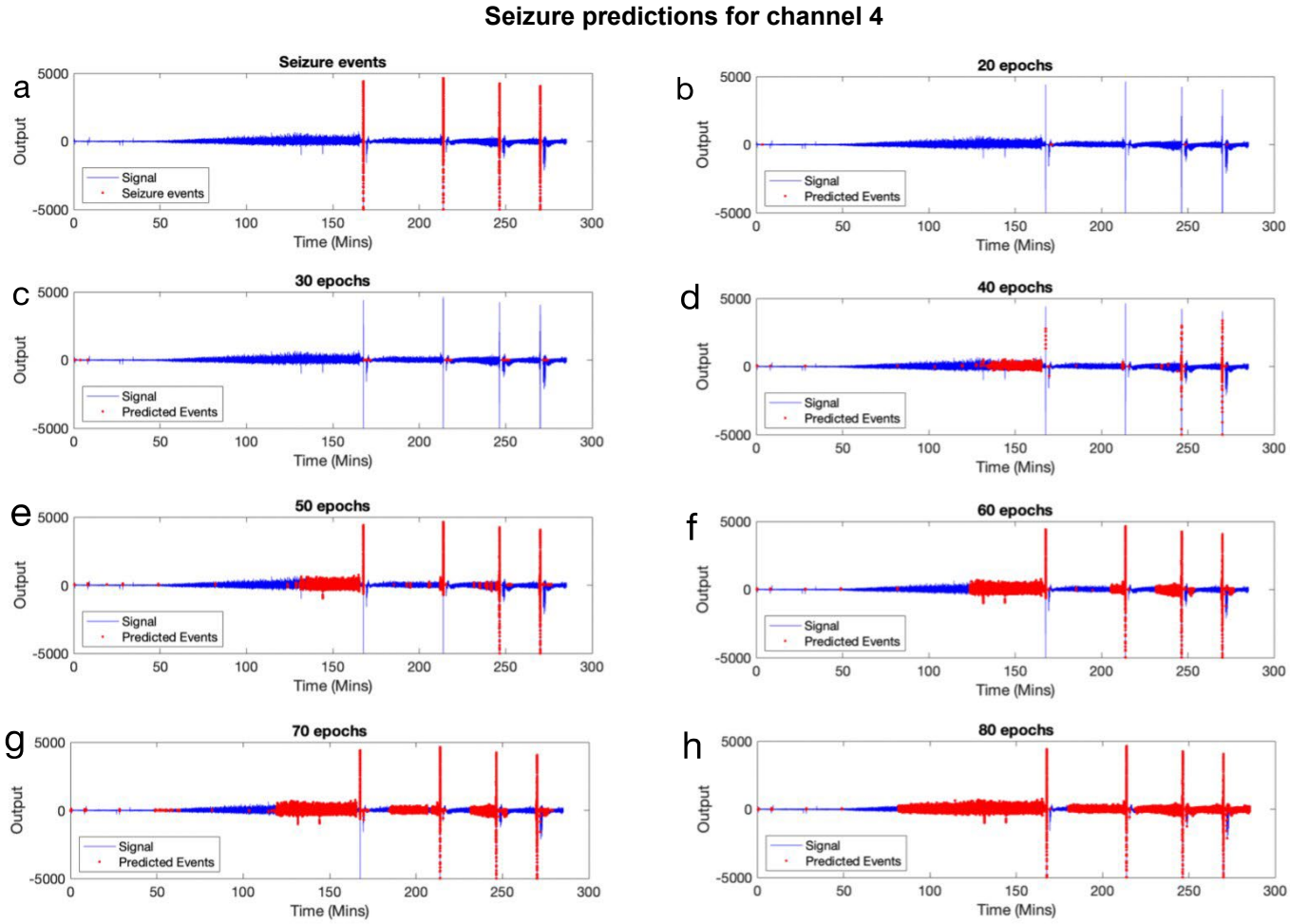

Figure. 11
Model performance for channel 4, using networks trained at an increasing number of epochs. Graph (a) shows channel 1 actual seizure events highlighted in red. (b) shows channel 1 tested at 20 epochs (c) at 30 epochs, (d) 40 epochs, (e) 50 epochs (f) 60 epochs (g) 70 epochs and (h) 80 epochs. Total number of seizure points in channel 4 is 3087.

Although the model with networks trained at 20 and 30 epochs did make some seizure predictions, these were delayed (Figure 9-11), resulting in FPs rather than TPs. This suggests that 20 and 30 epochs were insufficient for the model to learn the data and update its weights accordingly.
Channel 1 (Figure 9a) has nine seizure spikes which were all detected from 40 epochs onwards, although not all the individual data points along each seizure were detected. Channel 3 (Figure 10a) also has nine seizure spikes where 100% were also identified from 40 epochs onwards.
Channel 4 (Figure 11a) has the least number of seizures, with a total of four. Interestingly, unlike the other two channels, only 75% of the seizure spikes were identified at 40 epochs, with no points detected along the second spike. However, at 50 epochs, 100% of the seizure spikes were detected, demonstrating that 40-50 epochs are the ideal number of epochs needed for accurate seizure detection across the test channels. The model was later re-trained using 45 epochs (Figure 12) following the calculation of the performance metrics, and the results were amended to Table 1.

Performance metrics

	30 epochs	40 epochs	45 epochs	50 epochs	60 epochs	70 epochs	80 epochs
Channel 1	Accuracy:98.9% Sensitivity: 0% Specificity: 99.9% Precision: 0% F1 score: 0.0	Accuracy:97.9% Sensitivity: 50.7% Specificity: 98.5% Precision: 27.0% F1 score: 0.3	Accuracy: 95.4% Sensitivity: 64.2% Specificity: 95.6% Precision: 13.84% F1 score: 0.2	Accuracy:87.4% Sensitivity: 72.1% Specificity: 87.5% Precision: 5.9% F1 score: 0.1	Accuracy: 78.9% Sensitivity: 75.3% Specificity: 78.9% Precision: 3.7% F1 score: 0.1	Accuracy: 79.4% Sensitivity: 88.3% Specificity: 79.2% Precision: 4.4% F1 score: 0.1	Accuracy: 56.6% Sensitivity: 81.0% Specificity: 56.3% Precision: 1.96% F1 score: 0.0
Channel 3	Accuracy: 99.3% Sensitivity: 0% Specificity: 99.8% Precision: 0% F1 score: 0.0	Accuracy: 98.9% Sensitivity: 28.6% Specificity: 99.2% Precision: 15.4% F1 score: 0.2	Accuracy: 93.1% Sensitivity: 56.9% Specificity: 93.3% Precision: 4% F1 score: 0.1	Accuracy: 77.4% Sensitivity: 74.8% Specificity: 77.4% Precision: 1.6% F1 score: 0.0	Accuracy: 68.7% Sensitivity: 80.3% Specificity: 68.6% Precision: 1.2% F1 score: 0.0	Accuracy: 69.3% Sensitivity: 83.1% Specificity: 69.2% Precision: 1.3% F1 score: 0.0	Accuracy: 47.0% Sensitivity: 85.3% Specificity: 46.8% Precision: 0.8% F1 score: 0.0
Channel 4	Accuracy: 99.6% Sensitivity: 0% Specificity: 99.9% Precision: 0% F1 score: 0.0	Accuracy: 99.4% Sensitivity: 16.7% Specificity: 99.7% Precision: 18.4% F1 score: 0.2	Accuracy: 98.1% Sensitivity: 50% Specificity: 98.4% Precision: 9.6% F1 score: 0.2	Accuracy: 89.6% Sensitivity: 68.6% Specificity: 89.7% Precision: 2.4% F1 score: 0.0	Accuracy: 74.9 Sensitivity: 77.2% Specificity: 74.9% Precision: 1.1% F1 score: 0.0	Accuracy: 66.9% Sensitivity: 80.8% Specificity: 66.9% Precision: 0.01% F1 score: 0.0	Accuracy: 36.9% Sensitivity: 81.3% Specificity: 36.7% Precision: 0.5% F1 score: 0.0
All Channels	Accuracy: 99.3% Sensitivity: 0% Specificity: 99.9% Precision: 0% F1 score: 0.0	Accuracy: 98.8% Sensitivity: 38.7% Specificity: 99.2% Precision: 22.9% F1 score: 0.3	Accuracy: 95.5% Sensitivity: 59.7% Specificity: 95.8% Precision: 8.3% F1 score: 0.1	Accuracy: 84.8% Sensitivity: 72.1% Specificity: 84.9% Precision: 3.0% F1 score: 0.1	Accuracy: 74.2% Sensitivity: 76.9% Specificity: 74.2% Precision: 1.9% F1 score: 0.0	Accuracy: 71.9% Sensitivity: 85.6% Specificity: 71.8% Precision: 1.9% F1 score: 0.0	Accuracy: 46.8% Sensitivity: 82.1% Specificity: 46.6% Precision: 1% F1 score: 0.0

Table. 1 Performance metrics for the model. The LSTM model performance for seizure detection on all three test channels at an increasing number of training epochs (30 to 80). Accuracy, sensitivity, specificity, precision and the F1 score have been presented, and rounded to one decimal place. 20 epochs were not included as the results were almost identical to 30 epochs. The best score is highlighted for each performance measure for individual channels, to determine optimal number of epochs. An average of each of the channels has been taken to determine overall performance. Performance for 45 epochs has been amended to the table.

As epochs increase for all three channels accuracy decreases, sensitivity/recall increases, and specificity decreases (Table 1). Interestingly, for 70 epochs on channel 1, the results demonstrate a slight anomaly, as the accuracy and specificity slightly increase from 60 epochs to 79.4% and 79.2% respectively, before decreasing again at 80 epochs to 56.6% and 81%; this is also seen for channel 3 where accuracy and specificity increase from 60 epochs and decrease again at 80 epochs. The opposite effect is seen for sensitivity in channel 1 where the score decreases from 88.3% at 70 epochs to 81% at 80 epochs.
Sensitivity increases as the model detects more seizures out of the total number of seizure events. Sensitivity however does not consider the number of non-seizure events being misclassified as seizure events and therefore the model may have high sensitivity but also a more significant number of FP results. This is shown by the decrease in specificity which considers FPs.
Precision measures number of correct positive predictions. The greatest precision was seen at 40 epochs (Table 1), whereas 0% precision was seen for 30 epochs across all channels because no seizures were detected correctly, although false positives were seen (Figure 9-11). The precision was also lower at 80 epochs (1%) because although many seizures were predicted correctly, this was counteracted by the greater number of FPs detected, resulting from the class imbalance.

Accuracy was also reported alongside other metrics for comparison although it is not the best metric to use as it provides little value to our model performance evaluation because of its misleading nature on imbalanced datasets where it is biased towards the majority non-seizure class. This is evidenced by initial model testing where 30 epochs produced an average accuracy (Table 1) of 99.3% despite the plot demonstrating that seizures were not correctly predicted (Figure 9b-11b). Consequently, the F1 score was a more useful metric to determine model performance as it is the harmonic mean of precision and recall/sensitivity, making it the go-to metric for class imbalance problems and, therefore, making a model effective this number should be sought to be maximised. The greatest F1 score was seen at 40 epochs for all channels individually and combined (Table 1), suggesting that 40 epochs may be optimal for seizure detection in this model. Nevertheless, it would not be optimal for seizure detection in real application as an F1 score of 0.3 is poor and for a model that is vital to patients' safety and wellbeing an algorithm with a score this low would be unsuitable.
Due to the large difference in performance observed between 40 and 50 epochs (Table 1) in areas such as precision and sensitivity, the model was re-trained at 45 epochs and tested on all channels (Figure 12). Following the training at 45 epochs and a review of its performance (Table 1), the optimal number of epochs remained as 40 epochs, although at 45 epochs 100% of the seizure spikes were detected in channel 4 (Figure 12f). In contrast, at 40 epochs only three out of the four spikes were detected.

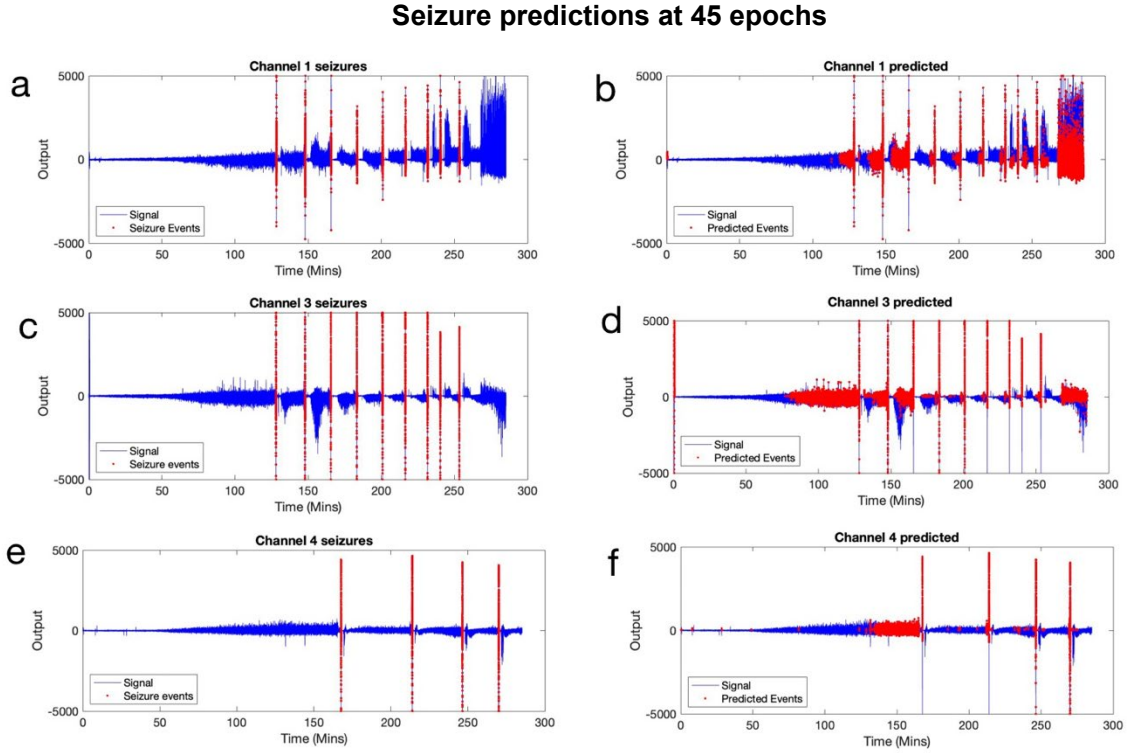

Figure 12.
Model performance for channel 1, 2 and 3, using a network trained at 45 epochs. (A) Graph shows channel 1 output with actual seizures in red (B) Predicted seizures for channel 1 (C) channel 3 output with actual seizures represented in red (D) channel 3 predicted seizures at 45 epochs, (e) channel 4 network output with seizure points highlighted in red and normal signal shown in blue, (f) channel 4 predicted seizures at 45 epochs.

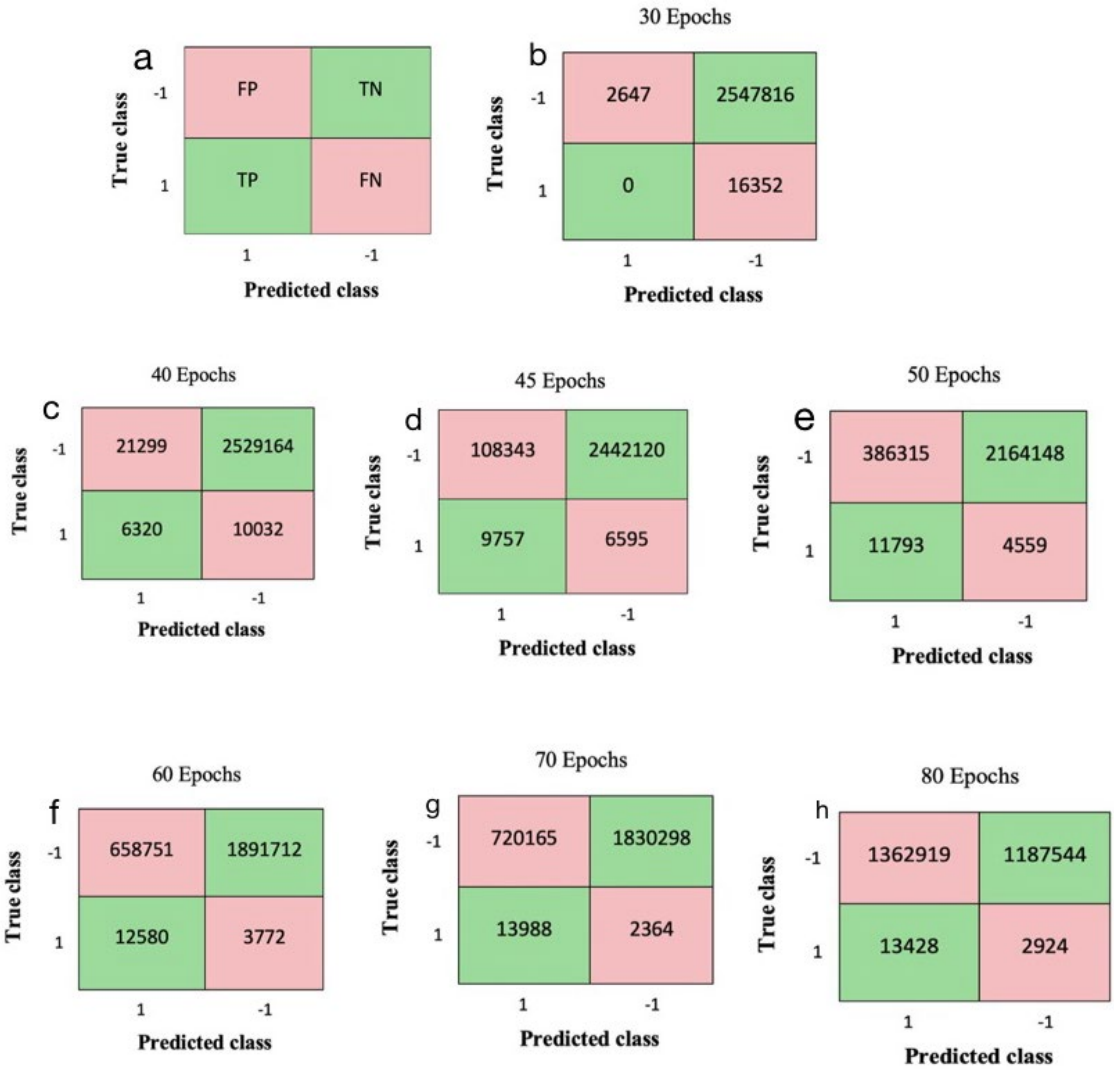

Table 2. Confusion matrices for combined test channels at an increasing number of epochs from 30 to 80. Total number of seizures points in the test sets combined were 16352, and total number of non-seizure points were 2550463. (A) shows FP, TP, TN, and FN for reference and 1 represents a seizure event while -1 represents non-seizures.

The confusion matrices demonstrate a clear trend (Table 2); as the number of epochs increases, the number of seizure points correctly detected increases but at the expense of a substantial number of non-seizures misclassified as seizure events. A slight anomaly is seen at 70 epochs where the number of TP is greater than at 80 epochs, as also observed in Table 1. There is also a considerable number of false negatives seen at 80 epochs compared to 70 epochs suggesting 80 epochs is not optimal for model performance. Although 40 epochs are most optimal in terms of the performance metrics for precision, F1 score, accuracy, and specificity (Table 1), the sensitivity was poor. This is demonstrated in Table 2c, where there are more TN than TP points. At 45 epochs, however, (d) the number of TPs in relation to TNs increased, while the model maintained specificity and accuracy to an acceptable degree (Table 1).

Discussion

A novel method for automatically detecting epileptic seizures has been developed. A model has been presented and evaluated using real test datasets for the first-time using LSTM and LFP data for seizure detection. The model was trained using a dataset with four seizure spike events and was subsequently presented with three unseen signals with a different number of seizures for testing. Considering the limited data, this model has demonstrated an impressive ability to detect seizures. However, we cannot be certain that the parameters selected for model training are, in fact, optimal due to the model's 'black box' nature. Although 40 epochs seem to be ideal for seizure detection (Table 1), the most optimal number of epochs may lie anywhere between 40-45.

Model performance across all test channels was similar; however, for significantly different datasets, the model performance would be varied, and there is no way to determine whether the model would be optimised in this same way without requiring further tuning of parameters. This is a disadvantage because a model would need to uphold performance across datasets to be applicable for real-life use. This difference is demonstrated on a small scale in channel 4, which had four seizure spikes in comparison to nine in the other two test channels. This may be why channel 4 could only detect 75% of seizures at 40 epochs, whilst the other two channels detected 100%. Therefore, it is essential to highlight that this model may not be appropriate to use and replicate for real-life seizure detection in its current state. It can further be hypothesised that performance is likely to have been different if the model was trained on a different channel. For example, channel 1 had the greatest number of seizure points with 9115. Consequently, channel 1 could offer an opportunity to train on a greater number of seizures than channel 2 (5946 seizure points), potentially making the model more effective by slightly reducing the impact of the class imbalance.

Literature review

Due to the variance in ML algorithms used, data collection methods, and difference in performance metrics used to evaluate models, a direct comparison with other studies is not possible. However, related studies have been reviewed and compared where possible. Based on 40 epochs, the LSTM algorithm in this study produced an accuracy of 98.8%, sensitivity of 38.7%, specificity of 99.2%, and precision of 22.9%. Ahmedt-Aristizabal and colleagues (2018) proposed a similar LSTM classifier for identifying healthy, interictal, and ictal EEG signals. Interestingly, their model achieved an average accuracy of 91.25%, sensitivity of 91.83%, specificity of 90.5%, and a high precision of 91.50%. Despite the model's greater accuracy and specificity, it was at the cost of significantly lower sensitivity and precision. This alludes that the model has not been optimised in the best way possible, and the algorithm needs to be improved before it can be considered a successful seizure prediction algorithm. As part of Ahmedt-Aristizabal's and colleagues' (2018) study, depth electrodes were implanted into the hippocampal formation to train the model on data from five TLE patients. Their dataset contained 100 samples, each with 4096 segments, but the number of points associated with each class was not described; thus, we cannot determine whether there was an imbalance among the classes. Their study included two network configurations, one with one LSTM layer and 64 hidden units and the other with two hidden layers, one with 128 and the other with 64 hidden units (Ahmedt-Aristizabal *et al*., 2018). Considering these differences, it is possible that increasing LSTM layers to two may have led to a better model since it allows the detection of complex features (Singh & Malhotra., 2022). In another study, Singh and Malhotra (2022) found that their model could detect seizures using two LSTM layers with an average accuracy of 98.14 %, a sensitivity of 98.51 %, and a specificity of 97.78 % using 200 training epochs.

Singh and Malhotra (2022) study showed a considerable increase in epochs from our study where 40 were optimal; however, Ahmedt-Aristizabal and coworkers (2018) only used 20 epochs to prevent overfitting while still achieving good performance. In this case, the number of epochs may not be the cause of the high accuracy. In addition, accuracy decreased notably at 80 epochs from 70 epochs (Table 1) and training the network with 80 epochs revealed overfitting at two points (Figure 8). This overfitting occurs when the model does not learn the characteristics of the data but memorises it, consequently struggling when given unseen data (IBM Cloud Education, 2020). Thus, it may be beneficial to increase LSTM layers to two in the future, although this will increase training time. While we observed differences between our study and that of Ahmedt-Aristizabal and coworkers

(2018), the LSTM was optimised in the same way with the Adam optimizer and a learning rate of 0.001. As such, we can suggest that the differences in performance might be attributable to the number of layers LSTM layers or the class imbalance in the present dataset.

Seizure classification

The high number of FPs demonstrated that this model is not acceptable, as we can have no confidence that a detected event is genuinely a seizure. A model such as this deployed for real-life applications could significantly impact patients and healthcare services relying on this device for accurate seizure detection and warning. FPs may lead to more people being admitted to the hospital, causing a strain on healthcare professionals' time and resources. Alternately, the excessive number of FPs could be considered an advantage clinically, as the seizures points are detected before they occur (Figure 9-11), which is essential for real-time warnings of a seizure. Therefore, it must be determined whether a higher sensitivity or specificity is more crucial as there may be situations where false detections are less problematic, and sensitivity is crucial.

The problem of excessive FPs arises because only seizure and non-seizure points have been labelled in the dataset. Therefore, the model is trained to detect the ictal event rather than pre-ictal events. For example, although 40 epochs seem to be optimal in terms of the performance measures, 50 – 60 epochs seem to be more effective in detecting pre-ictal phases of a seizure (Figure 9-11), although there is no way of knowing if these are accurate pre-ictal detections without labelling this phase as a separate class. Pre-ictal seizure detection has been shown in a study where Aghagolzadeh and colleagues (2016) demonstrated 80% accuracy, with no FPs using a CNN model. This suggests that labelling pre-ictal events would be beneficial to improve the model by reducing the number of false positives and therefore increasing precision, specificity, and accuracy. Researchers Rasekhi and colleagues (2013) implemented this strategy in greater depth by using four preictal times of 10, 20, 30, and 40 minutes, reporting that optimal preictal time is critical to achieving good seizure prediction results where they obtained an accuracy of 73.9%. Another drawback of our model is that it tests on individual channels without reporting latency of seizure detection (Burrello *et al*., 2021), which is an important metric for real-time seizure prediction as reported in a similar study utilising scalp and intracranial EEG; an average detection latency of 1.89 s with a 99.8% classification accuracy was reported (Vidyaratne and Iftekharuddin, 2017).

Furthermore, the model should be robustly tested on a dataset containing several artifacts to maintain model performance. For example, at the start of channel 3 an artifact was present and misclassified as a seizure from 40 epochs onwards (Figure 10). An algorithm proposed by Burrello and colleagues (2021) employing intracranial electroencephalography (iEEG) demonstrated that external noise and recording artifacts did not reduce the model's accuracy of 95.76%. Models capable of maintaining performance with artifacts present would be crucial because a real seizure detection device implementing this algorithm and recording in real-time from patients would need to be remain unaffected by common artifacts like blinking.

Limitations of the model

Although the LSTM model seems to be trained using a dataset of sufficient size, it is highly uneven due to the sparsity of seizures. The training set contained only 5946 seizure points in a dataset of 855,605, though it can be argued that a class imbalance reflects real-life recordings where there would be long recording durations with only a few seconds of seizure activity. The problem of unbalanced data has been addressed in a study (Yuan *et al*., 2017), where the minority seizure class in the dataset was assigned heavier weights using the weighted extreme learning machine. The model was able to produce a high sensitivity of 97.73% and specificity of 92.22%, which was not achieved in the LSTM model presented in this study as a high specificity meant that sensitivity was compromised and vice versa (Table 1*).* However, the weights assigned were not mentioned (Yuan *et al*., 2017), giving the reader a lack of insight into the true model parameters. Also, while assigning greater weights to a minority class may be beneficial, it could also cause the algorithm to become biased towards the minority class.

Another popular method of reducing class imbalance in machine learning is to re-sample the data by adding copies of the minority seizure class (oversampling) or deleting instances of the majority non-seizure class (undersampling). A synthetic minority oversampling algorithm has been applied

successfully to imbalanced EEG data for seizure detection by Hu and colleagues (2021), resulting in an average accuracy of 89.49%. The downside of oversampling is that, like assigning heavier weights, it might lead to bias towards the minority class and cause overfitting. Similarly, Amin and Kamboh (2016) analysed EEG for seizure prediction but exploited an under-sampling approach to solve the class imbalance. They achieved 97% accuracy using an SVM-based method, although the issue remains that under-sampling could lead to the loss of valid data. Researchers Shiao and colleagues (2017) further demonstrated the under-sampling approach in their study of canine epileptic seizures to develop a prediction algorithm. Their SVM-based system displayed a sensitivity between 90 and 100%, with daily false-positive rates between 0 and 0.3. Unfortunately, specificity and precision were not reported, and sensitivity alone provides an unrealistic evaluation of a model.
Therefore, it cannot be concluded if under-sampling was truly effective in this study.

Limitations of using animal models

A significant disadvantage of the algorithm developed is that it cannot be generalised to detect seizures using real-life recordings from epilepsy patients, considering that the model was trained using data collected from rats subjected to the RISE model of TLE. Although TLE is the most common type of epilepsy, so using TLE data would be sensible; epilepsy can be considered a spectrum disorder where it is multifaceted and varies between individuals (Sirven, 2017). Given that, seizure events can vary in other types of epilepsy, such as absence seizure epilepsy which presents with a 3Hz spike and wave on EEG recordings (Kakisaka *et al*., 2011). Thus, without further adaption, the model would be ineffective in detecting seizures in different types of epilepsies. Another disadvantage is that the model was trained using data from rats, so the direct application of the model to detect human seizures would not be appropriate. Norbert Wiener (1945) stated, “The best material model of a cat is another, or preferably the same, cat.” (Rosenblueth & Wiener, 1945). This quote refers to a model for detecting epileptic seizures in humans would be most effective if it included data from humans and ideally should be trained specifically for the target individual. However, this would take an inordinate amount of time, so weighing the risks and benefits would be practical.

The RISE model has several advantages over other epilepsy models, despite the criticisms mentioned above. This model of chronic TLE has a low mortality rate (1%) but high epileptogenic morbidity, where the emergence of spontaneous recurrent seizures distinguishes it following a relatively long seizure-free period (Modebadze *et al*., 2016). Despite the limitations of generalising animal models to humans, RISE replicates some of the core features of human TLE and epileptogenesis, such as variation in seizure frequency and intensity (Modebadze *et al*., 2016). Also, in contrast to kainate or pilocarpine animal models of epilepsy, which create apparent haemorrhages in many brain structures due to prolonged status epilepticus (Sloviter, 2005), the RISE model lacks neuronal damage, particularly to the CA3 recording area (Needs et al., 2019). As a result, we can have confidence that the model provides a realistic comparison of how a seizure detection device would perform in humans based on a model using these exact parameters.

Black box approach

LSTM is a 'black box' algorithm that is solely code, making it difficult to determine the reasons for an algorithm's performance and the individual classification steps involved (Fung *et al*., 2021). This can be problematic for datasets with a class imbalance, making it difficult to determine relationships between parameters, interpret results, and optimise model performance as it relies heavily on a trial-and-error process. "Non-black-box" or "white-box" classifiers are often more desirable as they are human-interpretable and explain each step of the process (Siddiqui *et al*., 2020), and recent studies have favoured random forests for seizure detection. In their 2017 paper, Siddiqui and colleagues compared two black-box models (SVM and KNN) for seizure detection and localisation with two white-box models (decision tree and decision forest). Their results exhibited that decision forests outperform black-box models by allowing epoch length reductions for quicker seizure detection without compromising accuracy. They also allow precise seizure localization -- a promising tool for epileptic surgery.

Conclusion

An accurate deep learning model of seizure detection holds the potential to revolutionise our understanding of epilepsy and its impacts on people's lives. This paper has demonstrated with preliminary results that epileptic seizures can be detected even in the early stages with an average accuracy of 98.8%, precision of 22.9%, and F1 score of 0.3. The proposed LSTM model's performance was evaluated and compared to other cutting-edge techniques mentioned in recent literature, where the novelty of this paper has been established in detecting LFP recorded seizures using an LSTM model. Although this work is a step in the right direction, successful detection of seizures from large volumes of brain recordings data remains a major challenge in epilepsy. Due to the complexity of such signals and epilepsy as a spectrum disorder, machine learning algorithms with appropriate classifiers and features are critical for high accuracy. This can be challenging because there is often a trade-off between using a black-box approach that often yields higher accuracy and a white-box approach that can be interpreted by humans and logically used to tune hyperparameters for a more optimal model.

The main improvements of this model would be the distinction between interictal and preictal states in the data processing stages, addressing the class imbalance at the outset, and more fine-tuning of the hyperparameters. In view of these improvements, it is plausible to suggest that the model with some improvement has the potential to be utilised for automatic seizure detection.

Using deep learning with spectrograms to classify epileptic seizure signals could be an upcoming objective. This would allow seizure detection in hours-long EEG recordings without consulting specialists, thus minimising human error and increasing accuracy. A tool such as this could be helpful in the diagnosis of epilepsy, speeding up the process and allowing for faster treatment.

To conclude, the LSTM network model is clearly a suitable technique for accurate and real-time prediction of epileptic seizures compared to other models. However, there is much room for improvement as the current model is not optimal or ready for any real-world application or hardware implementation. This is demonstrated by the performance metrics obtained by the model and a review of studies also utilising LSTM for automated seizure detection. In light of the numerous studies investigating machine learning for seizure detection, controlling epileptic seizures seems promising.

References

Abbasi, M.U., Rashad, A., Basalamah, A. and Tariq, M. (2019). Detection of Epilepsy Seizures in Neo-Natal EEG Using LSTM Architecture. *IEEE Access*, **7**: 179074–179085.

Aghagolzadeh, M., Hochberg, L. R., Cash, S. S., & Truccolo, W. (2016). Predicting seizures from local field potentials recorded via intracortical microelectrode arrays. *Annual International Conference of the IEEE Engineering in Medicine and Biology Society. IEEE Engineering in Medicine and Biology Society. Annual International Conference*, **2016**: 6353–6356.

Ahmedt-Aristizabal, D., Fookes, C., Nguyen, K. and Sridharan, S. (2018). *Deep Classification of Epileptic Signals*, **2018**: 332-335

Ali, R., Connolly, I.D., Feroze, A.H., Awad, A.J., Choudhri, O.A. and Grant, G.A. (2016). Epilepsy: A Disruptive Force in History. *World Neurosurgery*, **90**: 685–690.

Almustafa, K.M. (2020). Classification of epileptic seizure dataset using different machine learning algorithms. *Informatics in Medicine Unlocked*, 21: 100444.

Amin, S. and Kamboh, A.M. (2016). A robust approach towards epileptic seizure detection. *2016 IEEE 26th International Workshop on Machine Learning for Signal Processing (MLSP)*, **2016**: 1-6.

Anastasiadou, M., Hadjipapas, A., Christodoulakis, M., Papathanasiou, E.S., Papacostas, S.S. and Mitsis, G.D. (2014). Detection and Removal of Muscle Artifacts from Scalp EEG Recordings in Patients with Epilepsy. *2014 IEEE International Conference on Bioinformatics and Bioengineering*, **2014**: 291-296

Asanuma, M., S. Nishibayashi-Asanuma, I. Miyazaki, M. Kohno and N. Ogawa, 2001. Neuroprotective effects of non-steroidal anti-inflammatory drugs by direct scavenging of nitric oxide radicals. *Neurochemistry*, **76**: 1895-1904.

Beghi, E., Giussani, G. and Sander, J.W. (2015). The natural history and prognosis of epilepsy. *Epileptic disorders : international epilepsy journal with videotape*, **17(3)**: 243–53.

Beghi, E. and Giussani, G. (2018). Aging and the Epidemiology of Epilepsy. *Neuroepidemiology*, **51(3-4)**: 216–223.

Beghi, E. (2020). The Epidemiology of Epilepsy. *Neuroepidemiology*, **54(2)**: 185–191.

Bongiorni, L. and Balbinot, A. (2020). Evaluation of recurrent neural networks as epileptic seizure predictor. *Array*, **8**: 100038.

Brownlee, J. (2018). Difference Between a Batch and an Epoch in a Neural Network. [online] *Machine Learning Mastery*. Available at: https://machinelearningmastery.com/difference-between-a-batch-and-an-epoch/ [Accessed 11 April 2022]

Brownlee, J. (2019). Understand the Impact of Learning Rate on Neural Network Performance. [online] *Machine Learning Mastery*. Available at: https://machinelearningmastery.com/understand-the-dynamics-of-learning-rate-on-deep-learning-neural-networks/. [Accessed 21 April 2022]

Burrello, A., Benatti, S., Schindler, K., Benini, L. and Rahimi, A. (2021). An Ensemble of Hyperdimensional Classifiers: Hardware-Friendly Short-Latency Seizure Detection With Automatic iEEG Electrode Selection. *IEEE Journal of Biomedical and Health Informatics*, **25(4):** 935–946.

Buzsáki, G., Anastassiou, C.A. and Koch, C. (2012). The origin of extracellular fields and currents — EEG, ECoG, LFP and spikes. *Nature Reviews Neuroscience*, **13(6):** 407–420.

Chou, I-Ching., Wang, C.-H., Lin, W.-D., Tsai, F.-J., Lin, C.-C. and Kao, C.-H. (2016). Risk of epilepsy in type 1 diabetes mellitus: a population-based cohort study. *Diabetologia*, **59(6)**: 1196–1203.

Cutillo, C.M., Sharma, K.R., Foschini, L., Kundu, S., Mackintosh, M. and Mandl, K.D. (2020). Machine intelligence in healthcare—perspectives on trustworthiness, explainability, usability, and transparency. *Nature Publishing Group Digital Medicine*, **3(1)**: 1–5.

England, M.J., Liverman, C.T., Schultz, A.M. and Strawbridge, L.M. (2012). Epilepsy across the spectrum: Promoting health and understanding. *Epilepsy & Behavior*, **25(2)**: 266–276.

Englot, D.J., Nagarajan, S.S., Imber, B.S., Raygor, K.P., Honma, S.M., Mizuiri, D., Mantle, M., Knowlton, R.C., Kirsch, H.E. and Chang, E.F. (2015). Epileptogenic zone localization using magnetoencephalography predicts seizure freedom in epilepsy surgery. *Epilepsia*, **56(6):** 949–958.

Englot, D.J., Rolston, J.D., Wright, C.W., Hassnain, K.H. and Chang, E.F. (2016). Rates and Predictors of Seizure Freedom With Vagus Nerve Stimulation for Intractable Epilepsy. *Neurosurgery*, **79(3):** 345–353.

Fisher, R.S. (2017). The New Classification of Seizures by the International League Against Epilepsy 2017. *Current Neurology and Neuroscience Reports*, **17(6)**: 48.

Fisher, R.S., Scharfman, H.E. and deCurtis, M. (2014). How Can We Identify Ictal and Interictal Abnormal Activity? *Advances in Experimental Medicine and Biology*, **813**:3–23.

Fung, P.L., Zaidan, M.A., Timonen, H., Niemi, J.V., Kousa, A., Kuula, J., Luoma, K., Tarkoma, S., Petäjä, T., Kulmala, M. and Hussein, T. (2021). Evaluation of white-box versus black-box machine learning models in estimating ambient black carbon concentration. *Journal of Aerosol Science*, **152**: 105694.

Gagliano, L., Bou Assi, E., Nguyen, D.K. and Sawan, M. (2019). Bispectrum and Recurrent Neural Networks: Improved Classification of Interictal and Preictal States. *Scientific Reports*, **9(1)**: 15649.

Gaillard, F. (2020). Epoch (machine learning) | *Radiology Reference Article* | *Radiopaedia.org*. [online] Radiopaedia. Available at: https://radiopaedia.org/articles/epoch-machine-learning?lang=gb. [Accessed 21 April 2022]

Griffiths, M.J., Messent, M., MacAllister, R.J. and Evans, T.W. (1993). Aminoguanidine selectively inhibits inducible nitric oxide synthase. *British Journal of Pharmacology*, **110(3)**: 963–968.

Guo, L., Rivero, D., Dorado, J., Rabuñal, J.R. and Pazos, A. (2010). Automatic epileptic seizure detection in EEGs based on line length feature and artificial neural networks. *Journal of Neuroscience Methods*, **191(1)**: 101–109.

Henderson, C.B., Filloux, F.M., Alder, S.C., Lyon, J.L. and Caplin, D.A. (2006). Efficacy of the Ketogenic Diet as a Treatment Option for Epilepsy: Meta-analysis. *Journal of Child Neurology*, **21(3)**: 193–198.

Hillbom, M., Pieninkeroinen, I. and Leone, M. (2003). Seizures in alcohol-dependent patients: epidemiology, pathophysiology and management. *CNS drugs*, **17(14**): 1013–30.

Hochreiter, S. and Schmidhuber, J. (1997). Long Short-Term Memory. *Neural Computation*, **9(8)**: 1735–1780.

Hu, D., Cao, J., Lai, X., Liu, J., Wang, S. and Ding, Y. (2021). Epileptic Signal Classification Based on Synthetic Minority Oversampling and Blending Algorithm. *IEEE Transactions on Cognitive and Developmental Systems*, **13(2)**: 368–382.

Hunyadi, B., Siekierska, A., Sourbron, J., Copmans, D. and de Witte, P.A.M. (2017). Automated analysis of brain activity for seizure detection in zebrafish models of epilepsy. *Journal of Neuroscience Methods*, 287: 13–24.

Hussein, R., Palangi, H., Wang, Z.J. and Ward, R. (2018). Robust Detection of Epileptic Seizures Using Deep Neural Networks. *2018 IEEE International Conference on Acoustics, Speech and Signal Processing (ICASSP)*, **2018**: 2546-2550

IBM Cloud Education (2020). *What are Neural Networks?* [online] www.ibm.com. Available at: https://www.ibm.com/uk-en/cloud/learn/neural-networks [Accessed 28 March 2022].

Katzner S, Nauhaus I, Benucci A, Bonin V, Ringach DL, Carandini M. (2009). Local origin of field potentials in visual cortex. *Neuron* **61**: 35– 41.

Kakisaka, Y., Alexopoulos, A.V., Gupta, A., Wang, Z.I., Mosher, J.C., Iwasaki, M. and Burgess, R.C. (2011). Generalized 3-Hz spike-and-wave complexes emanating from focal epileptic activity in pediatric patients. *Epilepsy & Behavior*, **20(1)**: 103–106.

Lekshmy, H.O., Panickar, D. and Harikumar, S. (2022). Comparative analysis of multiple machine learning algorithms for epileptic seizure prediction. *Journal of Physics: Conference Series*, **2161(1)**: 2055.

Lu, E., Pyatka, N., Burant, C.J. and Sajatovic, M. (2021). Systematic Literature Review of Psychiatric Comorbidities in Adults with Epilepsy. *Journal of Clinical Neurology*, **17(2)**: 176.

MacDonald, J.F., Bartlett, M.C., Mody, I., Pahapill, P., Reynolds, J.N., Salter, M.W., Schneiderman, J.H. and Pennefather, P.S. (1991). Actions of ketamine, phencyclidine and MK-801 on NMDA receptor currents in cultured mouse hippocampal neurones. *The Journal of Physiology*, **432(1)**: 483–508.

Manford, M. (2017). Recent advances in epilepsy. *Journal of Neurology*, **264(8)**: 1811–1824.

Maragatham, G. and Devi, S. (2019). LSTM Model for Prediction of Heart Failure in Big Data. Journal of Medical Systems, **43(5)**: 111.

Matejka, J. (2020). Why Research Is Needed | *Epilepsy Research UK*. [online] epilepsyresearch.org.uk. Available at: https://epilepsyresearch.org.uk/our-research/why-research-is-needed/ [Accessed 22 April 2022].

Mitzdorf, U. (1985). Current source-density method and application in cat cerebral cortex: investigation of evoked potentials and EEG phenomena. *Physiological Reviews*, **65(1)**: 37–100.

Mlinar, S., Petek, D., Cotič, Ž., Mencin Čeplak, M. and Zaletel, M. (2016). Persons with Epilepsy: Between Social Inclusion and Marginalisation. *Behavioural Neurology*, **2016**: 2018509

Modebadze, T., Morgan, N.H., Pérès, I.A.A., Hadid, R.D., Amada, N., Hill, C., Williams, C., Stanford, I.M., Morris, C.M., Jones, R.S.G., Whalley, B.J. and Woodhall, G.L. (2016). A Low Mortality, High Morbidity Reduced Intensity Status Epilepticus (RISE) Model of Epilepsy and Epileptogenesis in the Rat. *PLoS ONE*, **11(2)**. e0147265.

Needs, H.I., Henley, B.S., Cavallo, D., Gurung, S., Modebadze, T., Woodhall, G. and Henley, J.M. (2019). Changes in excitatory and inhibitory receptor expression and network activity during

induction and establishment of epilepsy in the rat Reduced Intensity Status Epilepticus (RISE) model. *Neuropharmacology*, **158**: 107728.

Ngugi, A.K., Bottomley, C., Kleinschmidt, I., Sander, J.W. and Newton, C.R. (2010). Estimation of the burden of active and life-time epilepsy: A meta-analytic approach. *Epilepsia*, **51(5)**: 883–890.

Panteliadis, C.P., Vassilyadi, P., Fehlert, J. and Hagel, C. (2017). Historical documents on epilepsy: From antiquity through the 20th century. *Brain & Development*, **39(6)**: 457–463.

Patel, P. and Moshé, S.L. (2020). The evolution of the concepts of seizures and epilepsy: What's in a name? *Epilepsia Open*, **5(1)**: 22–35.

Peng, W., Cotrina, M.L., Han, X., Yu, H., Bekar, L., Blum, L., Takano, T., Tian, G.-F., Goldman, S.A. and Nedergaard, M. (2009). Systemic administration of an antagonist of the ATP-sensitive receptor P2X7 improves recovery after spinal cord injury. *Proceedings of the National Academy of Sciences*, **106(30)**: 12489–12493.

Proctor, P.H. (2008). Uric Acid: Neuroprotective or Neurotoxic? *Stroke*, **39(5)**: 88.

Pugliatti, M., Beghi, E., Forsgren, L., Ekman, M. and Sobocki, P. (2007). Estimating the Cost of Epilepsy in Europe: A Review with Economic Modeling. *Epilepsia*, **48(12):**2224-2233

Rasekhi, J., Mollaei, M.K., Bandarabadi, M., Teixeira, C. and Dourado, A. (2015). Epileptic seizure prediction based on ratio and differential linear univariate features. *Journal of Medical Signals & Sensors*, **5(1)**: 1.

Reynolds, E.H. (2009). Milestones in epilepsy. *Epilepsia*, **50(3)**: 338–342.

Rosenblueth, A. and Wiener, N. (1945). The Role of Models in Science. *Philosophy of Science*, **12(4)**: 316–321.

Rowe, M. (2019). An Introduction to Machine Learning for Clinicians. *Academic Medicine*, **94(10)**:1433-1436

Ryu, S. and Joe, I. (2021). A Hybrid DenseNet-LSTM Model for Epileptic Seizure Prediction. *Applied Sciences*, **11(16)**: 7661.

Schmidt, D. and Schachter, S.C. (2014). Drug treatment of epilepsy in adults. *British Medical Journal*, 28: **348**

Shiao, H.-T., Cherkassky, V., Lee, J., Veber, B., Patterson, E.E., Brinkmann, B.H. and Worrell, G.A. (2017). SVM-Based System for Prediction of Epileptic Seizures from iEEG Signal. *IEEE transactions on bio-medical engineering*, **64(5)**: 1011–1022.

Shoeibi, A., Khodatars, M., Ghassemi, N., Jafari, M., Moridian, P., Alizadehsani, R., Panahiazar, M., Khozeimeh, F., Zare, A., Hosseini-Nejad, H., Khosravi, A., Atiya, A.F., Aminshahidi, D., Hussain, S.,

Rouhani, M., Nahavandi, S. and Acharya, U.R. (2021). Epileptic Seizures Detection Using Deep Learning Techniques: A Review. *International Journal of Environmental Research and Public Health*, **18(11)**: 5780.

Siddiqui, M.K., Islam, M.Z. and Kabir, M.A. (2017). Analyzing Performance of Classification Techniques in Detecting Epileptic Seizure. *Advanced Data Mining and Applications*, **2017**: 386–398.

Siddiqui, M.K., Morales-Menendez, R., Huang, X. and Hussain, N. (2020). A review of epileptic seizure detection using machine learning classifiers. Brain Informatics, **7(1)**: 5.

Singh, K. and Malhotra, J. (2022). Two-layer LSTM network-based prediction of epileptic seizures using EEG spectral features. *Complex & Intelligent Systems*.

Sirven, J.I. (2015). Epilepsy: A Spectrum Disorder. *Cold Spring Harbor Perspectives in Medicine*, **5(9)**: 022848.

Sloviter, R.S. (2005). The neurobiology of temporal lobe epilepsy: too much information, not enough knowledge. *Comptes Rendus Biologies*, **328(2)**: 143–153.

Smith, S.J.M. (2005). EEG in the diagnosis, classification, and management of patients with epilepsy. *Journal of Neurology, Neurosurgery & Psychiatry*, **76(2)**, 2–7.

Sone, D. and Beheshti, I. (2021). Clinical Application of Machine Learning Models for Brain Imaging in Epilepsy: A Review. *Frontiers in Neuroscience*, **15**: 684825

Stacey, W.C. and Litt, B. (2008). Technology Insight: neuroengineering and epilepsy—designing devices for seizure control. *Nature clinical practice. Neurology*, **4(4)**: 190–201.

Stafstrom, C.E. and Carmant, L. (2015). Seizures and Epilepsy: An Overview for Neuroscientists. *Cold Spring Harbor Perspectives in Medicine*, **5(6)**, 022426–022426.

Steinlein, O.K. (2008). Genetics and epilepsy. *Epilepsy and Psychiatry*, **10(1)**: 29–38.

sudep.org. (n.d.). *SUDEP Action* | Making every epilepsy death count. [online] Available at: https://sudep.org/.

Tang, J., El Atrache, R., Yu, S., Asif, U., Jackson, M., Roy, S., Mirmomeni, M., Cantley, S., Sheehan, T., Schubach, S., Ufongene, C., Vieluf, S., Meisel, C., Harrer, S. and Loddenkemper, T. (2021). Seizure detection using wearable sensors and machine learning: Setting a benchmark. *Epilepsia*, **62(8)**, 1807–1819.

Tellez-Zenteno, J. and Nguyen, R. (2009). Injuries in epilepsy: a review of its prevalence, risk factors, type of injuries and prevention. *Neurology International*, **1(1)**: 20.

Usman, S.M., Usman, M. and Fong, S. (2017). Epileptic Seizures Prediction Using Machine Learning Methods. *Computational and Mathematical Methods in Medicine*, **2017**: 1–10.

Vidyaratne, L.S. and Iftekharuddin, K.M. (2017). Real-Time Epileptic Seizure Detection Using EEG. *IEEE Transactions on Neural Systems and Rehabilitation Engineering*, **25(11)**: 2146–2156.

West, S., Nevitt, S.J., Cotton, J., Gandhi, S., Weston, J., Sudan, A., Ramirez, R. and Newton, R. (2019). Surgery for epilepsy. *Cochrane Database of Systematic Reviews*. **25**: 6

World health organization (2019). *Epilepsy*. [online] World Health Organization. Available at: https://www.who.int/news-room/fact-sheets/detail/epilepsy. [Accessed 14 April 2022]

Wright, S.K., Rosch, R.E., Wilson, M.A., Upadhya, M.A., Dhangar, D.R., Clarke-Bland, C., Wahid, T.T., Barman, S., Goebels, N., Kreye, J., Prüss, H., Jacobson, L., Bassett, D.S., Vincent, A., Greenhill, S.D. and Woodhall, G.L. (2020). In vitro characterisation and neurosteroid treatment of an N-Methyl-D-Aspartate receptor antibody-mediated seizure model.

Yasrab, R., Pound, M.P., French, A.P. and Pridmore, T.P. (2020). PhenomNet: Bridging Phenotype-Genotype Gap: A CNN-LSTM Based Automatic Plant Root Anatomization System.

Yuan, Q., Zhou, W., Zhang, L., Zhang, F., Xu, F., Leng, Y., Wei, D. and Chen, M. (2017). Epileptic seizure detection based on imbalanced classification and wavelet packet transform. *Seizure*, **50**: 99–108.

Zare, M., Nazari, M., Shojaei, A., Raoufy, M.R. and Mirnajafi-Zadeh, J. (2020). Online analysis of local field potentials for seizure detection in freely moving rats. *Iranian journal of basic medical sciences*, **23(2)**: 173–177.

Appendices

Please find below the source code for training and testing the model in MATLAB. Testing scripts were modified to work with networks trained at several epochs, and in this example, 'net45' corresponds to 45 epochs.

```
%% Training script

% Load in data
load('0190_channel2_input(1) (1).mat')
load('0190_channel2_output(1) (1).mat')

channel2_section=channel2;
channel2_output_section=channel2_output;

% Convert Time for x_axis
timepoint = 285.2/855605;
time = [timepoint:timepoint:timepoint*855605];

% Create Plot with Seizures highlighted
plot(time, channel2_section, 'b')
hold on
plot(time(channel2_output_section==1),channel2_section(channel2_output_section==1), 'r')
xlabel('Time (ms)')
ylabel('Signal')
title('Local field potential with seizure events')

% Define Model
numFeatures=1;
numHiddenUnits=200;
numClasses=2;
layers = [...
    sequenceInputLayer(numFeatures)
    lstmLayer(numHiddenUnits, 'OutputMode','sequence')
    fullyConnectedLayer(numClasses)
    softmaxLayer
    classificationLayer];
options =trainingOptions("adam",...
    "MaxEpochs",45,...
    "GradientThreshold", 2,...
    "Verbose",0,...
    "Plots",'training-progress')

% Train the network
net = trainNetwork(channel2',categorical(channel2_output)',layers,options);
save('net45','net')
```

```
%% Testing Script (Channel 1)

% Load network
load('net45.mat')

% Load channel 1
load('0190_channel1_input(1) (2).mat')
load('0190_channel1_output(1) (2).mat')

% Transpose the data
channel1=channel1';

% Convert output to categorical
output1=categorical(channel1_output);

% Classify the test data
YPred = classify(net,channel1)';
YPred_numerical=double(YPred);
YPred_numerical(YPred_numerical==1)=1;
YPred_numerical(YPred_numerical==2)=-1;

% Calculate the accuracy of the predictions
acc = sum(YPred == output1)./numel(output1)

% Time for x_axis
timepoint = 285.2/855605;
time = [timepoint:timepoint:timepoint*855605];

% Create Plot with Seizures highlighted
figure(1)
subplot(3,2,1)
plot(time, channel1, 'b')
hold on
plot(time(channel1_output==1),channel1(channel1_output==1), '.r')
xlabel('Time (Mins)')
ylabel('Output')
title('Channel 1 Seizures')
legend('Signal', 'Seizure Events', 'Location','southwest')

subplot(3,2,2)
plot(time, channel1, 'b')
hold on
plot(time(YPred=='1'),channel1(YPred=='1'), '.r')
xlabel('Time (Mins)')
ylabel('Output')
title('Channel 1 Prediction')
legend('Signal', 'Predicted Events', 'Location','southwest')

% Confusion matrix
figure
confusionchart(channel1_output,YPred_numerical)
```

```
%% Testing Script (Channel 3)

% Load channel 3
load('0190_channel3_input(1).mat')
load('0190_channel3_output(1).mat')

% Transpose the data
channel3=channel3';

% Convert output to categorical
output3=categorical(channel3_output);

% Classify the test data
YPred = classify(net,channel3)';
YPred_numerical=double(YPred);
YPred_numerical(YPred_numerical==1)=1;
YPred_numerical(YPred_numerical==2)=-1;

% Calculate the accuracy of the predictions
acc = sum(YPred == output3)./numel(output3);

% Time for x_axis
timepoint = 285.2/855605;
time = [timepoint:timepoint:timepoint*855605];

% Create Plot with Seizures highlighted
figure(1)
subplot(3,2,3)
plot(time, channel3, 'b')
hold on
plot(time(channel3_output==1),channel3(channel3_output==1), '.r')
xlabel('Time (Mins)')
ylabel('Output')
title('Channel 3 Seizures')
legend('Signal', 'Seizure events','Location','southwest')

subplot(3,2,4)
plot(time, channel3, 'b')
hold on
plot(time(YPred=='1'),channel3(YPred=='1'), '.r')
xlabel('Time (Mins)')
ylabel('Output')
title('Channel 3 Prediction')
legend('Signal', 'Predicted Events','Location','southwest')

% Confusion matrix
figure
confusionchart(channel3_output, YPred_numerical)
```

```
%% Testing Script (Channel 4)

% Load channel 4
load("0190_channel4_input(1) (1).mat")
load("0190_channel4_output(1).mat")

% Transpose the data
channel4=channel4';

% Convert output to categorical
output4=categorical(channel4_output);

% Classify the test data
YPred = classify(net,channel4)';
YPred_numerical=double(YPred);
YPred_numerical(YPred_numerical==1)=1;
YPred_numerical(YPred_numerical==2)=-1;

% Calculate the accuracy of the predictions
acc = sum(YPred == output4)./numel(output4)

% Time for x_axis
timepoint = 285.2/855605;
time = [timepoint:timepoint:timepoint*855605];

% Create Plot with Seizures highlighted
figure(1)
subplot(3,2,5)
plot(time, channel4, 'b')
hold on
plot(time(channel4_output==1),channel4(channel4_output==1), '.r')
xlabel('Time (Mins)')
ylabel('Output')
title('Channel 4 Seizures')
legend('Signal', 'Seizure events', 'Location','southwest')

subplot(3,2,6)
plot(time, channel4, 'b')
hold on
plot(time(YPred=='1'),channel4(YPred=='1'), '.r')
xlabel('Time (Mins)')
ylabel('Output')
title('Channel 4 Prediction')
legend('Signal', 'Predicted Events', 'Location','southwest')

% % Confusion matrix
figure
confusionchart(channel4_output,YPred_numerical)

% Calculate the number of points corresponding to seizures
Seizure_points=sum(channel4_output==1);
Corresponding_output=double(YPred_numerical(channel4_output==1));
Number_of_correctly_predicted_points=sum(Corresponding_output==-1);
Accuracy=Number_of_correctly_predicted_points/Seizure_points;
```